Chapter 7: Summary, Mechanistic Aspects, Literature reported catalysts and Future Scope of Work

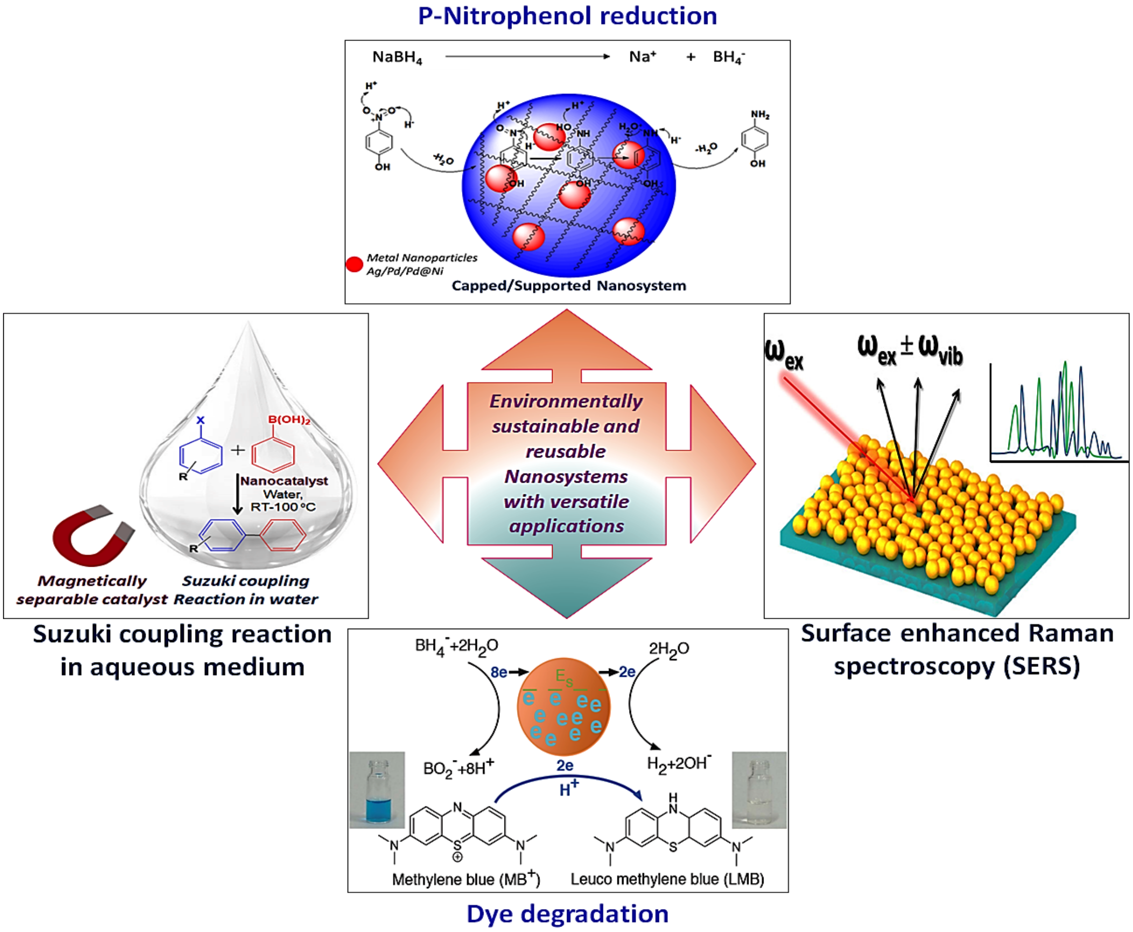

7.1. Performance evaluation of nanosystems under study

7.1.1. Chitosan stabilized nanosystems

Chitosan supported silver nanoparticles (Ag@Ch), Magnetic Iron Oxide nanoparticles (IO-Chitosan, IO-DTPA and IO-DTPA-DNA), Palladium based mono metallic Magnetic nanosystem (Pd@IO-Chitosan, Pd@IO-DTPA and Pd@IO-DTPA-DNA) and Pd and Ni based bimetallic magnetic nanosystems (Pd@Ni@IO-Chitosan and Pd@Ni@IO-DTPA) were prepared. Fabricated nanoparticles were characterised by various techniques like IR, SEM, EDX, HRTEM, XRD, XPS, XANES, VSM, TGA, ESR and STEM-HAADF techniques.

Nanostructures comprising of silver nanoparticles supported on chitosan (Ag@Ch) were successfully synthesized. It was confirmed that Silver is present in the form of Ag(0) and Ag_2O in Rhombus shaped silver nanoparticles. Nanoclusters of silver provided hotspots for SERS enhancement and was effective for sensing aqueous solutions of methylene blue (MB) dye, Crystal Violet (CV) dye and p-Nitrophenol (p-NP) with detection limits of 3.8, 8.1 and 8.2 ppb respectively. The SERS enhancement of the Ag@Ch was attributed to the combination of both electromagnetic (EM) and chemical effects (CE). Density functional theory (DFT) calculations were used to explain the observed surface enhancement. Good agreement was observed between the experimental and simulated spectra.

Palladium-based Monometallic and Bimetallic nanocatalyst supported on magnetic chitosan (Pd@IO-Chitosan & Pd@Ni@IO-Chitosan) were synthesized and used for Suzuki Miyaura C-C coupling reaction and p-Nitrophenol reduction reaction.

Use of Ni based chitosan or Ni based DTPA as support has increased the palladium content in the catalyst than the use of pristine supports without Ni.

The catalysts (Pd@IO-Chitosan & Pd@Ni@IO-Chitosan) comprised Pd, PdO, Pd^{2+} species stabilised by chitosan that facilitated Suzuki coupling reactions with excellent yields of over 99%. Pd@IO-Chitosan could be recycled and reused at least 12 times and 26 times with no significant decrease in its catalytic activity for Suzuki coupling and p-NP reduction respectively. Introducing Nickel atoms into the catalyst improved the catalytic activity as a result of synergistic effect between Ni and Pd. Magnetic saturation has incresed from 52.91emu/g (Pd@IO-Chitosan) to 74.38 emu/g (Pd@Ni@IO-Chitosan) as confirmed from VSM spectra. The Pd@Ni@IO-Chitosan shows excellent catalytic activity with high TON and could be reused upto 17 cycles for Suzuki coupling reaction and 31 cycles for p-Nitrophenol reduction.

The increasing use of palladium in the field of catalysis, energy, and environmental applications has motivated the development of efficient processes for its separation and reuse. Glyoxal crosslinked chitosan derivative (GCC) was used to adsorb Palladium from synthetic electroless plating solutions. Penta twinned icosahedron of palladium could be fabricated by gradual adsorption of palladium onto GCC. Quantitative adsorption of Pd^{2+} was achieved independent of pH conditions (1-10) in 120 minutes using 0.2 g of GCC. The adsorbent loaded with Pd was evaluated for its catalytic potential towards Suzuki coupling reaction, p-Nitrophenol reduction and dye degradation contributing to environmental sustainability.

7.1.2. DTPA stabilized nanosystems

Magnetic Diethylenetriaminepentaacetic acid (DTPA) stabilized Palladium nanostructures (Pd@IO-DTPA and Pd@Ni@IO-DTPA) were prepared and well characterised with various techniques. Superparamagnetic nanosystems were prepared with particle size ranging from 5-30 nm containing Pd in the form of Pd(0), Pd^{2+} and PdO. Prepared catalysts were further applied for p-Nitrophenol reduction and Suzuki coupling reaction in aqueous system. These catalysts could be easily isolated by simple handheld magnet and reused further for next consecutive cycles. Pd@IO-DTPA was recycled upto six cycles for Suzuki coupling reaction and 21 cycles for p-NP reduction. Similarly, Pd@Ni@IO-DTPA was recycled upto 13 and 29 cycles for Suzuki coupling reaction and p-NP reduction respectively.

7.1.3. DNA stabilized nanosystems

Pd@IO-DTPA showed good catalytic activity with least recyclability, due to the palladium leaching and aggregation. Therefore, we stabilized nanosystem (Pd@IO-DTPA) with one more bio inspired molecule and prepared DNA based hybrid palladium nanosystem (Pd@IO-DTPA-DNA) and checked its catalytic activity for Suzuki coupling reaction and p-NP reduction. This catalyst showed an excellent catalytic performance with very high recyclability. It showed recyclability upto 19 cycles for Suzuki coupling and 32 times for p-NP reduction.

Table 7.1 summarizes the Pd/Ni composition, shape and saturation magnetization values of the catalyst systems under study.

The bimetallic systems had higher magnetization values as compared to monometallic due to presence of Nickel in both chitosan and DTPA systems. Pd@IO-DTPA-DNA possessed highest magnetization value. Pd@IO-DTPA had higher magnetization value as compared to chitosan system.

Table 7.1: wt% of Pd/Ni from EDS, Particle size from HRTEM, Ms values from VSM and Amount of Pd^0, Pd^{2+} and PdO present in synthesized palladium based Nanosystems from XPS

Nanosystems	**EDS**	**HRTEM**	**VSM**	**XPS**		
	Wt% of Pd/Ni	**Particle shape and size**	**Ms value (emu/g)**	**Pd^0 (%)**	**Pd^{2+} (%)**	**PdO (%)**
Chitosan based magnetic catalytic system						
IO-Chitosan	-	Spherical (5-20 nm)	52.91	-		
Pd@IO-Chitosan	0.94 wt% Pd	Spherical (5-15 nm)	39.037	47.24	-	52.76
Ni@IO-Chitosan	-	Spherical + rod (5-20 nm)	81.07	-		
Pd@Ni@IO-Chitosan	0.79 wt% Ni, 2.09 wt% Pd	Spherical + rod (5-18 nm)	74.38	35.15	32.32	32.53
Chitosan based nonmagnetic catalytic system						
GCC-Pd	3.56 wt% Pd	Icosahedron (24-30 nm)	-	54.12	45.88	-
DTPA based magnetic catalytic system						
IO-DTPA	-	Spherical (15-25 nm)	67.20	-		
Pd@IO-DTPA	0.71 wt% Pd	Spherical (15-30 nm)	64.948	42.17	36.2	21.63
Ni@IO-DTPA	-	Spherical (7-15 nm)	78.06	-		
Pd-Ni@IO-DTPA	0.72 wt% Ni, 1.20 wt% Pd	Spherical (8-25 nm)	75.43	28.95. 5.87%Pd(Ni)		45.17
DNA based magnetic catalytic system						
IO-DTPA-DNA	-	Spherical	76.001			
Pd@IO-DTPA-DNA	2.62 wt% Pd	Core shell (6-18 nm)	73.92	48.08	51.76	

7.2. Application of Nanosystems under study for Suzuki coupling reaction in aqueous system

The presence of Pd^0, PdO and Pd^{2+} as active catalytic species makes Pd Nanosystems an effective catalyst for suzuki coupling wherein it could be recycled and reused for many cycles thus increasing the TON. The TON was calculated as mol product / per mol Pd and when taking into account the number of cycles the catalyst can be reused the formula mol product* cycles/ per mol Pd was used. It was observed from the results that:

1. Use of DTPA as a capping resulted in the use of trace amount of base (0.1-0.5 equivalent) for C-C coupling reactions. And it showed good catalytic activity with K_2CO_3, Na_2CO_3, KOH, and NaOH. While, Chitosan stabilized nanocatalyst were effective with K_2CO_3, Na_2CO_3.
2. Stability and recyclability of chitosan supported nanosystem is more than the DTPA stabilized nanosystem.
3. TON of DTPA stabilized systems were higher than chitosan based systems wherein the monometallic systems had higher values as compared to bimetallic systems.
4. The TOF values were found to be higher for DTPA system than chitosan system wherein the values were higher for bimetallic systems
5. It was observed from elemental analysis that loading of Pd has increased in case of Ni@IO-Chitosan than the IO-Chitosan due to which reaction time has decreased in case of Pd@Ni@IO-Chitosan. Therefore, TOF of Pd@Ni@IO-Chitosan (3394.57 h^{-1}) was observed to be higher than the Pd@IO-Chitosan (3083.33 h^{-1}). Pd@IO-Chitosan showed high yield (>99%) with higher TON (18500) than Pd@Ni@IO-Chitosan (TON 10500) under mild conditions.
6. . The TON of Pd@IO-DTPA and Pd@Ni@IO-DTPA are 23800 and 17857.14 respectively. The TOF Pd@IO-DTPA and Pd@Ni@IO-DTPA are 3404.46 h^{-1} and 3571.42 h^{-1}. These high TON & TOF values could be attributed to the high distribution of palladium nanoparticles on the support which permits them to have direct interaction with the reaction substrate. As a result, palladium utilization ratio increases and TON/TOF values increases
7. Rate of reaction was increased in reaction catalyzed by Bimetallic nanosystem.
8. Stability of the DTPA capped nano catalyst has increased after capping with DNA and high recyclability was achieved.
9. A general summary of Pd-based heterogeneous catalysts reported in literature for Suzuki coupling reactions has been tabulated. (Table 7.2). However, it is difficult to

compare the efficacy of the catalyst based on TON and TOF due to the different conditions used and methodology adapted for calculation. Highest TON values are reported in literature for palladacycles (10^6-10^7) and the TON of present nanosystems under study were of the order of 10^4 for one cycle and 10^5 when the number of cycles are taken into account. (Gautam & Bhanage, 2015)

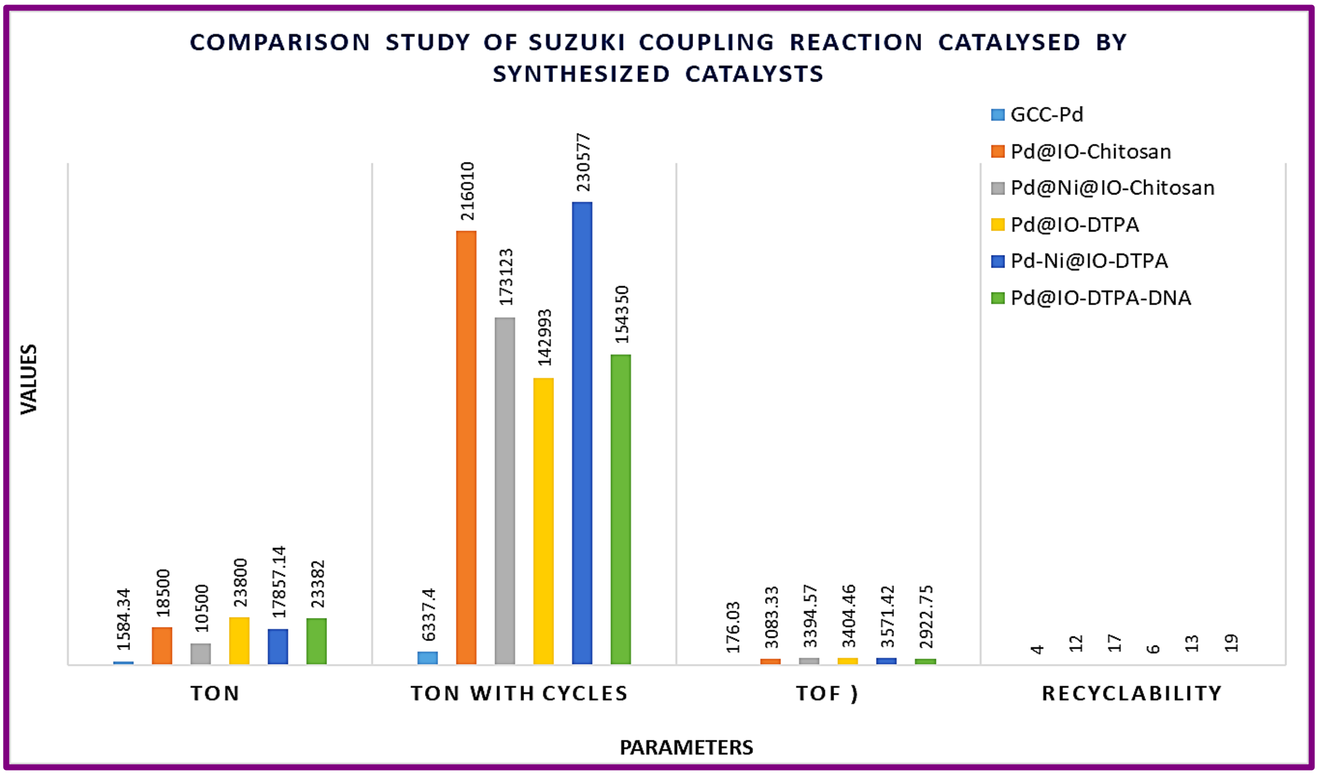

Figure 7.1 Comparison study of Suzuki coupling reaction catalysed by synthesized catalytic systems; Reaction conditions: *Iodobenzene (1.59-2 mmol), Phenylboronic acid (1.59-2 mmol), catalyst dose:1 mg, solvent (10 ml water), Base-* K_2CO_3 (0.5-2 equi.), *TLC (n-hexane), GC-MS (HPLC grade chloroform*

The possible reaction mechanism of Suzuki cross-coupling reactions

A plausible mechanism involved for monometallic Palladium nanoparticles is (Begum et al., 2017; Chen et al., 2007) (Figure 7.2A). Characterization studies such as XPS, XRD, HRTEM indicated that both Pd(II) and Pd(0) were present in Synthesized Pd based nanocatalysts facilitating oxidative addition and recycling of the catalyst.

1. A plausible mechanism is shown in the scheme 1 for the Suzuki coupling reaction based on (Pd(0)/Pd(II) couple). Firstly, Pd(0) present in the catalyst underwent oxidative addition of aryl

halide to generate an aryl-palladium complex (Ar-Pd-X) wherein Pd(0) is oxidized to Pd (II). (**Oxidative addition**)

The transformation may be through heterogeneous pathway wherein the charged palladium nanoparticles present in catalyst can participate in the oxidative addition. The formed Pd(II) after oxidative addition and Pd(II) present in catalyst can catalyse the rest of the cycle (Begum et al., 2017; Chen et al., 2007)

2. (Ar-Pd-X) couples with phenylboronic acid in the presence of a base (K_2CO_3) to produce an intermediate complex (Ar-Pd^{II}-Ph) (**trans metalation**)

3. Finally it forms the biaryl product via the reductive elimination of metallic palladium (**Reductive elimination**)

In the case of Ni-Pd bimetallic nanosystem (Figure 7.2B), the charge transfer from Ni to Pd, makes Pd less positively charged which provides a favorable site for facile oxidative addition of aryl halides and hence enhanced catalytic activity for Ni–Pd nanoparticle catalysts. in the last step of the cyclic mechanism, part of the Ni in the Pd–Ni alloy undergoes de-alloying and because standard reduction potential of $Pd^{2+/}$Pd0 (0.83 V) is higher than that of Ni^{2+}/Ni^0 (−0.23 V), therefore Ni transfers electrons to Pd(II) and eventually metallic Pd regenerates.

Considering our experimental results, only the Ni NP (Ni@IO-DTPA and Ni@IO-Chitosan) shows no significant catalytic activity. However, its use with Pd helps to maintain similar activity in subsequent cycles because Ni sacrifices electrons to the oxidized Pd (Bao et al., 2019). Since the Pd content after each consecutive cycle remained almost similar, the recyclability of the catalyst in the coupling reaction is higher than the monometallic Pd catalysts.

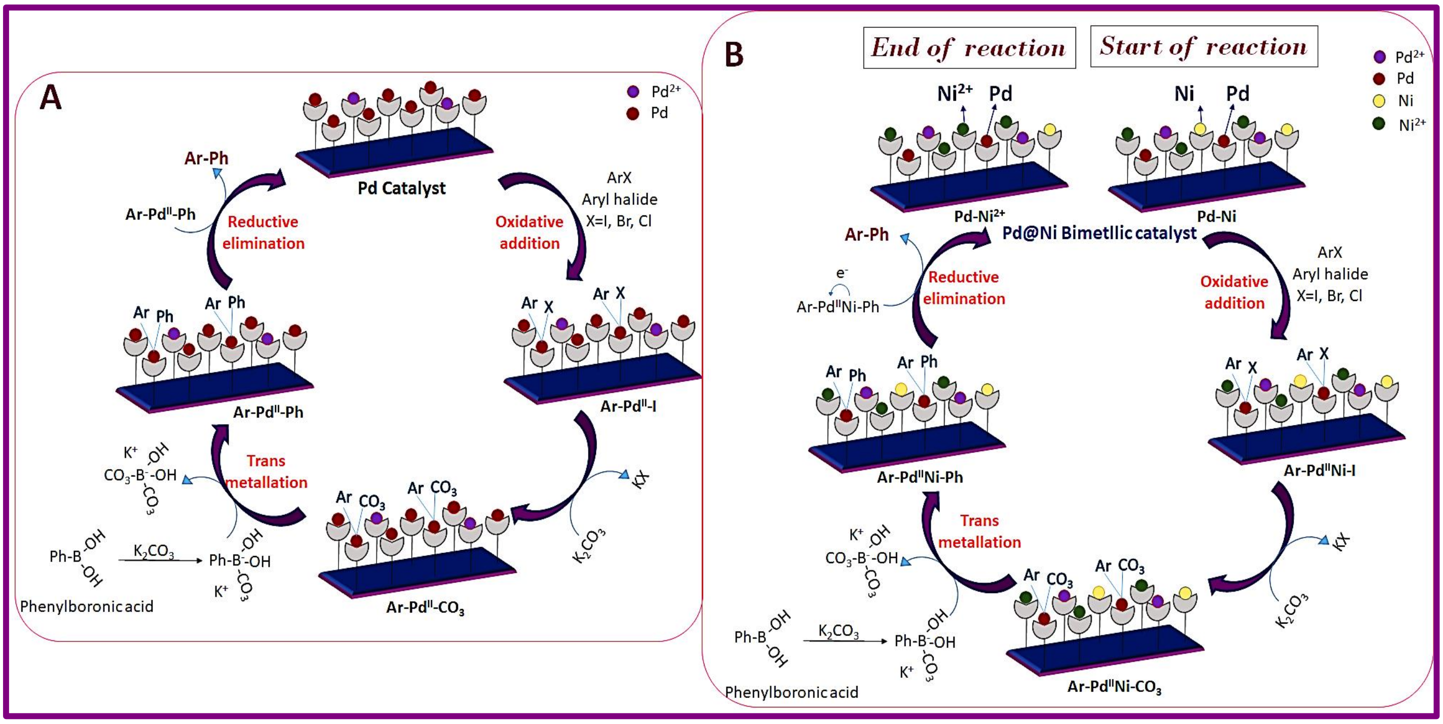

Figure 7.2: *Plausible mechanism from Suzuki coupling reaction catalysed by monometallic Pd nanosystem*

Table 7.2: Comparison table of Suzuki coupling reaction catalysed by synthesized catalyst

Sr. No.	Catalyst	Reaction Condition	TON/TOF	Recycl ability	References
1	Double-shelled hollow nanospheres supported Pd nanoparticles,	Starting materials: Iodobenzene (0.5 mmol), Phenylboronic acid (1.0 mmol); Catalyst: 5 mg; Time: 90 min; Solvent: ethanol; Temp: 78 °C; Conversion: 99.9%	TOF: 52.7 min^{-1}	-	(Duan et al., 2018)
2	Palladium nanoparticles immobilized on a magnetic Chitosan-anchored Schiff base (0.02 mol% Pd)	Starting materials: Bromobenzene (1.0 mmol), Phenylboronic acid (1.0 mmol); Time: 30 min; Solvent: PEG-200: H_2O (1:1); Temp: 50 °C; Conversion:99%	TON:4950	5	(Anuradha et al., 2017)
		Starting materials: chlorobenzene (1.0 mmol), Phenylboronic acid (1.0 mmol); Time: 3h; Solvent: PEG-200: H_2O (1:1); Temp: 50 °C; Conversion:99%	TON:4950		
3	Pd nanoparticles modified silica support (0.2 g)	Starting materials: Iodobenzene (2 mmol), Phenylboronic acid (2.4 mmol); Time: 3h; Solvent: H_2O; Temp:80 °C; Conversion:99%	TOF: 272.29 h^{-1}		(Online et al., 2016)
4	Palladium nanocubes (2 mg)	Starting materials: Iodobenzene (0.27 mmol), phenylboronic acid (0.30 mmol); Time: 30 min; Solvent: EtOH: H_2O (1:1) (5 mL); Temp: 50 °C; Conversion:95%	TON: 1242	5	(Swain et al., 2020a)
		Starting materials: Bromobenzene (0.27 mmol), Phenylboronic acid (0.30 mmol); Time: 60 min; Solvent: EtOH: H_2O (1:1) (5 mL); Temp: 50 °C; Conversion:92%	TON: 1563		
5	Palladium complex stabilized on functionalized polymeric support (20 mg)	Starting materials: p-Bromobenzaldehyde (1 mmol), Phenylboronic acid (1 mmol); Time: 90 min; Solvent: Ethanol: H_2O (2:2 mL); Temp: reflux: Conversion:95%	TON: 226	5	(Ariannezhad et al., 2022)
6	$PdCl_2$ loaded on tartaric acid modified magnetite nanoparticles (20 mg)	Starting materials: Iodobenzene (1 mmol), Phenylboronic acid (1 mmol); Time: 20 min; Solvent: Ethanol: H_2O (1:1); Temp: 75 °C; Conversion:99%	-	5	(Amirmahani et al., 2021)
		Starting materials: Bromobenzene (1 mmol), Phenylboronic acid (1 mmol); Time: 20 min; Solvent: Ethanol: H_2O (1:1); Temp: 75 °C; Conversion:95%			
7	Palladium(II) nanomagnetic catalyst	Starting materials: Iodobenzene (1 mmol), Phenylboronic acid (1.2 mmol); Time: 1 h; Solvent: DMF: H_2O (8:2); Temp:80 °C; Conversion:96%	TON: 342 TOF: 342 h^{-1}	5	(Vibhute et al., 2020)

		Starting materials: Chlorobenzene (1 mmol), Phenylboronic acid (1.2 mmol); Time: 3 h; Solvent: DMF: H_2O (8:2); Temp:80 °C; Conversion:86%	TON: 317 TOF: 102 h^{-1}		
8	Palladium (II) anchored to the silica MCM-41	Starting materials: Iodobenzene (1 mmol), Phenylboronic acid (1 mmol); Time: 15 min; Solvent: Ethanol/ H_2O; Temp: 80°C; Conversion:97%	-	8	(Molaei & Ghadermazi, 2021)
		Starting materials: Bromobenzene (1 mmol), Phenylboronic acid (1 mmol); Time: 30 min; Solvent: Ethanol/ H_2O; Temp: 80°C; Conversion:95%			
		Starting materials: Chlorobenzene (1 mmol), Phenylboronic acid (1 mmol); Time: 6 h; Solvent: Ethanol/ H_2O; Temp: 80°C; Conversion:60%			
		Starting materials: 4-Iodotoluene (1 mmol), Phenylboronic acid (1 mmol); Time: 60 min; Solvent: Ethanol/ H_2O; Temp: 80°C; Conversion:96%			
		Starting materials: 2-Iodotoluene (1 mol), Phenylboronic acid (1 mmol); Time: 30 min; Solvent: Ethanol/ H_2O; Temp: 80°C; Conversion:92%			
9	Pd(II)-Pd(0) anchored to magnetic nanoparticles (Fe_3O_4) on biguanidine-chitosan polymer (0.20 mol% Pd);	Starting materials: Iodobenzene (1 mmol), Phenyl boronicacid (1.1 mmol) Base: K_2CO_3 (2 mmol), Solvent: H_2O-EtOH, Temp: 25 °C; Time 1 h: Conversion: 96%	-	7	(Veisi et al., 2018)
		Starting materials: 1-Iodo-4-methylbenzene (1 mmol), Phenyl boronicacid (1.1 mmol) Base: K_2CO_3 (2 mmol); Solvent: H_2O-EtOH, Temp: 25 °C; Time: 2 h, conversion: 96%			
		Starting materials: Bromobenzene (1 mmol), Phenyl boronicacid (1.1 mmol) Base: K_2CO_3 (2 mmol), Solvent: H_2O-EtOH, Temp: 25 °C, Time: 2 h, conversion: 96%			
		Starting materials: Chlorobenzeene (1 mmol), Phenyl boronicacid (1.1 mmol) Base: K_2CO_3 (2 mmol), Solvent: H_2O-EtOH, Temp: 25 °C, Time: 24 h, conversion: 40%			
10	Pd nanoparticles supported on chitosan-encapsulated Fe_3O_4/SiO_2-NH_2 nanoparticles (0.1 mol%):	Starting materials: Iodobenzene (1 mmol), Phenyl boronicacid (1 mmol), Base: K_2CO_3 (2 mmol), Solvent: H_2O: EtOH, Temp: 40 °C, Time: 0.25 h, conversion: 98%	-	8	(Veisi et al., 2020)
		Starting materials: 1-Iodo-4-methylbenzene (1 mmol), Phenyl boronicacid (1 mmol), Base: K_2CO_3 (2 mmol), Solvent: H_2O: EtOH, Temp: 40 °C, Time: 0.5 h, conversion: 98%			

		Starting materials: Bromobenzene (1 mmol), Phenyl boronicacid (1 mmol), Base: K_2CO_3 (2 mmol), Solvent: H_2O: EtOH, Temp: 40 °C, Time: 0.5 h, conversion: 96%			
		Starting materials: Chlorobenzene (1 mmol), Phenyl boronicacid (1 mmol), Base: K_2CO_3 (2 mmol), Solvent: H_2O: EtOH, Temp: 40 °C; Time: 5 h, conversion: 60%			
11	Pd nanoparticles on magnetic chitosan: (0.004 mol% Pd);	Starting materials: Iodobenzene (1 mmol), Phenyl boronicacid (1.1 mmol), Base: KOH (2 mmol), Solvent: EtOH, Temp: Room temperature; Time: 20 min; Conversion 97%	-	4	(Hajipour et al., 2017)
		Starting materials: Bromobenzene (1 mmol), Phenyl boronicacid (1.1 mmol), Base: KOH (2 mmol), Solvent: EtOH, Temp: Room temperature Time: 20 min; Conversion:93%			
		Starting materials: Chlorobenzene (1 mmol), Phenyl boronicacid (1.1 mmol), Base: KOH (2 mmol), Solvent: EtOH, Temp: Room temperature; Time: 20 min; Conversion:43%			
12	Palladium nanoparticles on the surface modified magnetic Chitosan using methyl salicylate (0.10 mol% Pd);	Starting materials: Iodobenzene (1 mmol); Phenyl boronicacid (1.1 mmol) ;Base: K_2CO_3 (2 mmol) ; Solvent: EtOH:Water (4:1); Temp:80 °C; Time: 1h; Conversion: 98%	TON: 980 TOF: 980 h^{-1}	7	(Hasan, 2020)
		Starting materials: 1-Iodo-4-methylbenzene (1 mmol); Phenyl boronicacid (1.1 mmol); Base: K_2CO_3 (2 mmol); Solvent: EtOH:Water (4:1); Temp:80 °C; Time: 1h; Conversion: 96%			
		Starting materials: Bromobenzene (1 mmol); Phenyl boronicacid (1.1 mmol); Base: K_2CO_3 (2 mmol); Solvent: EtOH:Water (4:1); Temp:80 °C; Time: 2h; Conversion: 90%			
		Starting materials: Chlorobenzene (1 mmol); Phenyl boronicacid (1.1 mmol); Base: K_2CO_3 (2 mmol); Solvent: EtOH:Water (4:1); Temp:80 °C; Time: 8h; Conversion: 25%			
13	Magnetic-functionalized-multi-walled carbon nanotubes@chitosan N-heterocyclic carbene-palladium (0.1 mol%);	Starting materials: Iodobenzene (1 mmol), Aryl boronicacid (1.2 mmol), Base (K_2CO_3 2-3 mmol), solvent: (H_2O-EtOH: 1:1), Temp.: 40 °C; Time: 2h; Conversion: 100%	TON: 970 TOF: 485	5	(Sedghi et al., 2019)
		Starting materials: 1-Iodo-4-methylbenzene (1 mmol), Aryl boronicacid (1.2 mmol), Base (K_2CO_3 2-3 mmol), solvent: (H_2O-EtOH: 1:1), Temp.: 40 °C; Time: 2h; Conversion: 100%	TON: 970 TOF: 485		

		Starting materials: Bromobenzene (1 mmol), Aryl boronicacid (1.2 mmol), Base (K_2CO_3 2-3 mmol), solvent: (H_2O-EtOH: 1:1), Temp.: 40 °C; Time: 3h; Conversion: 97%	TON: 939 TOF: 313		
		Starting materials: Chlorobenzene (1 mmol), Aryl boronicacid (1.2 mmol), Base (K_2CO_3 2-3 mmol), solvent: (H_2O-EtOH: 1:1), Temp.: 60 °C; Time: 8h; Conversion: 55%	TON: 52.8 TOF: 6.6		
14	Pd nanoparticles (Pd NPs) were decorated on the magnetic nanocomposite consisting of chitosan/δ-FeOOH microspheres (0.05 mol%);	Starting materials: 1-Iodo-4-methylbenzene (1 mmol), Aryl boronicacid (1.5 mmol), Base (K_2CO_3 2.5 mmol), solvent: (H_2O-EtOH: 1:1), Temp.: (70 °C); Time: 3h; Conversion: 90%	TON: 1800 TOF: 600	8	(Melike Çalışkan & Baran, 2021)
15	Fe_3O_4@chitosan-bound 5-bromosalicylaldehyde Pd magnetic nanocatalyst (10 mg)	Starting materials: Iodobenzene (1 mmol), Phenyl boronicacid (1.2 mmol), Base: K_2CO_3 (1.5 mmol), Solvent: PEG; Temp: 80 °C; Time: 10 min; conversion:93%	-	4	(Fakhri & Naghipour, 2017)
		Starting materials: 1-Iodo-4-methylbenzene (1 mmol), Phenyl boronicacid (1.2 mmol), Base: K_2CO_3 (1.5 mmol), Solvent: PEG; Temp: 80 °C; Time: 75 min; conversion:94%			
		Starting materials: Bromobenzene (1 mmol), Phenyl boronicacid (1.2 mmol), Base: K_2CO_3 (1.5 mmol), Solvent: PEG; Temp: 80 °C; Time: 30 min; conversion:94%			
		Starting materials: Chlorobenzene (1 mmol), Phenyl boronicacid (1.2 mmol), Base: K_2CO_3 (1.5 mmol), Solvent: PEG; Temp: 80 °C; Time: 50 min; conversion:90%			
16	Core–shell type Magnetic Fe_3O_4@CS-Schiff base Pd (2-Pyridine carboxaldehyde): 10 mg	Starting materials: Iodobenzene (1 mmol); Phenyl boronic acid (1.2 mmol); Base: K_2CO_3 (1.5 mmol); Solvent: PEG; Temp: 80 °C; Time: 10min; Conversion:98%	-	5	(Naghipour & Fakhri, 2016)
		Starting materials: 1-Iodo-2-methylbenzene (1 mmol); Phenyl boronic acid (1.2 mmol); Base: K_2CO_3 (1.5 mmol); Solvent: PEG; Temp: 80 °C; Time: 60 min; Conversion: 95%			
		Starting materials: Aryl Halide (1 mmol); Phenyl boronic acid (1.2 mmol); Base: K_2CO_3 (1.5 mmol); Solvent: PEG; Temp: 80 °C; Time: 30 min; Conversion: 98%			
		Starting materials: Aryl Halide (1 mmol); Phenyl boronic acid (1.2 mmol); Base: K_2CO_3 (1.5 mmol); Solvent: PEG; Temp: 80 °C; Time: 20 min; Conversion: 98%			

		Starting materials: Aryl Halide (1 mmol); Phenyl boronic acid (1.2 mmol); Base: K_2CO_3 (1.5 mmol); Solvent: PEG; Temp: 80 °C; Time: 35 min; Conversion: 95%			
17	Palladium nanoparticles loaded on magnetic methionine functionalized chitosan (0.14 mol% Pd)	Starting materials: 1-Iodo-4-methylbenzene (0.5 mmol); Phenyl boronicacid (0.5 mmol); TBAB: (0.25 mmol), Base: K_2CO_3 (1 mmol); Solvent: water; Temp: RT; Time: 30 min; Conversion: 98%	-	10	(Abdol R. Hajipour & Tavangar-Rizi, 2017)
		Starting materials: Chlorobenzene (0.5 mmol); Phenyl boronicacid (0.5 mmol); TBAB: (0.25 mmol), Base: K_2CO_3 (1 mmol); Solvent: water; Temp: RT; Time: 120 min; Conversion: 85%			
18	Palladium nanoparticles decorated on the chitosan-activated carbon composites (0.0015 mmol)	Starting materials: Aryl Halide (1 mmol); Phenyl boronicacid (1.8 mmol); Base: K_2CO_3 (3.5 mmol); Temp: 400 W; Time: 6 min; Conversion:79%	-	10	(T. Baran, 2019)
		Starting materials: Aryl Halide (1 mmol); Phenyl boronicacid (1.8 mmol); Base: K_2CO_3 (3.5 mmol); Temp: 400 W; Time: 6 min; Conversion:69%			
19	Palladium nanoparticles stabilized on magnetically separable chitosan/agar microcapsules microcapsules) (0.015 mmol)	Starting materials: 1-Iodo-4-methylbenzene (1 mmol); Phenyl boronicacid (1.8 mmol); Base: K_2CO_3 (3.5 mmol); Temp: 400 W; Time: 5 min; Conversion:80%	-	10	(T. Baran & Nasrollahzadeh, 2019)
20	Cross-linked Chitosan (glutaraldehyde or diglycidyl ether) polyethylene glycol - supported palladium(0) catalyst: (0.50 mol%);	Starting materials: Iodobenzene (0.5 mmol); Phenyl boronicacid (0.75 mmol); Base: K_3PO_4 (1.5 mmol); Solvent: H_2O (TBAB (0.5 mmol); Temp: microwave (150 °C): Time: 15 min; Conversion: 87%	-	5	(Yi et al., 2007)
		Starting materials: 1-Iodo-4-methylbenzene (0.5 mmol); Phenyl boronicacid (0.75 mmol); Base: K_3PO_4 (1.5 mmol); Solvent: H_2O (TBAB (0.5 mmol); Temp: microwave (150 °C): Time: 15 min; Conversion:70%			
		Starting materials: 4-Iodobezaldehyde (0.5 mmol); Phenyl boronicacid (0.75 mmol); Base: K_3PO_4 (1.5 mmol); Solvent: H_2O (TBAB (0.5 mmol); Temp: microwave (150 °C): Time: 15 min; Conversion:95%			
21	Chitosan-g-mPEG-supported palladium (0) catalyst (mPEG: methoxy polyethylene glycol): (0.5 mol%);	Starting materials: Iodobenzene (0.5 mmol); Phenyl boronicacid (0.75 mmol); Base: K_2CO_3 (mmol); Solvent: water; Temp: 150 °C; Time: 0.33 h; Conversion:92%	-	5	(Sin et al., 2010)

		Starting materials: 1-Iodo-4-methylbenzene (0.5 mmol); Phenyl boronicacid (0.75 mmol); Base: K_2CO_3 (mmol); Solvent: water; Temp: 150 °C; Time: 3 h; Conversion:66%			
		Starting materials: Bromobenzene (0.5 mmol); Phenyl boronicacid (0.75 mmol); Base: K_2CO_3 (mmol); Solvent: water; Temp: 150 °C; Time: 2 h; Conversion:79%			
		Starting materials: Chlorobenzene (0.5 mmol); Phenyl boronicacid (0.75 mmol); Base: K_2CO_3 (mmol); Solvent: water; Temp: 150 °C; Time: 3 h; Conversion:13%			
22	Palladium Nanoparticles Doped on the Chitosan Nanofibers Modified using 2-Amino benzaldehyde	Starting materials: Iodobenzene (1 mmol); Phenyl boronicacid (1.2 mmol); Base: KOH (2 mmol); Solvent: H_2O: EtOH (2:1), Temp: (100 °C); Time: 15 min; Conversion: 96%	-	5	(Shahbazi & Bahrami, 2020)
23	Chitosan/ starch composite as support material for stabilization of palladium nanoparticles (0.005 mol% Pd);	Starting materials: 1-Iodo-4-methylbenzene (1.12 mmol); Phenyl boronicacid (1.87 mmol); Base: K_2CO_3 (3.75 mmol); Solvent free, Temp: (50 °C) microwave irradiation; Time: 0.1 h; Conversion: 75%	TON: 15000	7	(T. Baran et al., 2017)
		Starting materials: 1-Iodo-2-methylbenzene (1.12 mmol); Phenyl boronicacid (1.87 mmol); Base: K_2CO_3 (3.75 mmol); Solvent free, Temp: (50 °C) microwave irradiation; Time: 0.1 h; Conversion: 55%	TON: 11000		
24	Pd supported on chitosan-Schiff base ligand. ((Schiff base ligand: (4-aminobenzenesulfonic acid) and 2,6-diacetylpyridine)) (0.01 mol% Pd)	Starting materials: 1-Iodo-2-methylbenzene (1.12 mmol); Phenyl boronicacid (1.87 mmol); Base: K_2CO_3 (3.75 mmol); Solvent free, Temp: microwave irradiation (400 W); Time: 4 min; Conversion: 54%	TON: 5700	10	(T. Baran & Tulden Inanan Ayfer Mentes, 2016)
25	Palladium nanocatalyst on chitosan-cellulose composite (0.004 mol% Pd);	Starting materials: 1-Iodo-4-methylbenzene (1.12 mmol); Phenyl boronicacid (1.87 mmol) Base: K_2CO_3 (3.75 mmol); Solvent free, Temp: (50 °C) microwave irradiation; Time: 5 min; Conversion: 72%	TON: 18000	8	(N. Y. Baran et al., 2018)
		Starting materials: 1-Iodo-2-methylbenzene (1.12 mmol); Phenyl boronicacid (1.87 mmol) Base: K_2CO_3 (3.75 mmol); Solvent free, Temp: (50 °C) microwave irradiation; Time: 5 min; Conversion:60%	TON: 15000		

26	2,2′-Pyridil cross-linked chitosan based Pd(II) catalyst (0.0005 mol%);	Starting materials: 1-Iodo-4-methylbenzene (1.12 mmol); Phenyl boronicacid (1.75 mmol) Base: K_2CO_3 (3.75 mmol); Solvent free, Temp: (50 °C) microwave irradiation 400W; Time: 5 min; Conversion:33%	TON: 13800	7	(T. Baran et al., 2016)
		Starting materials: 1-Iodo-2-methylbenzene (1.12 mmol); Phenyl boronicacid (1.75 mmol) Base: K_2CO_3 (3.75 mmol); Solvent free, Temp: (50 °C) microwave irradiation 400W; Time: 5 min; Conversion:33%	TON: 6600		
27	Pd Immobilized on stabilizing agent [OCMCS-SB] produced from chitosan (OCMCS-SB-Pd(II)) [OCMCS-SB: Chitosan+vanillin+monochloroacetic acid] (0.46 mol% Pd);	Starting materials: Iodobenzene (0.5 mmol); aryl boronicacid (0.75 mmol) Base: K_2CO_3 (1 mmol); Solvent: Ethanol: water (3:2), Temp: (50 °C); Time:1.5h ; Conversion: 99%	-	5	(Dong et al., 2021)
		Starting materials: Bromobenzene (0.5 mmol); aryl boronicacid (0.75 mmol) Base: K_2CO_3 (1 mmol); Solvent: Ethanol: water (3:2), Temp: (50 °C); Time: 2h; Conversion:96%			
		Starting materials: Chlorobenzene (0.5 mmol); aryl boronicacid (0.75 mmol) Base: K_2CO_3 (1 mmol); Solvent: Ethanol: water (3:2), Temp: (50 °C); Time: 3.5h; Conversion:25%			
28	Magnetic Zeolite Y−Palladium−Nickel Ferrite (0.015 mol%)	Starting materials: Bromobenzene and Phenylboronic acid; Solvent: H_2O: Ethanol (1:1); Temperature: 80 °C; Time:1 h; Conversion: 96%	-	8	(Dehghani et al., 2019)
		Starting materials: Iodobenzene and Phenylboronic acid; Solvent: H_2O: Ethanol (1:1); Temperature: 80 °C; Time:0.5 h; Conversion: 99%			
		Starting materials: Chlorobenzene and Phenylboronic acid; Solvent: H_2O: Ethanol (1:1); Temperature: 80 °C; Time: 2 h; Conversion: 83%			
		Starting materials: 4-Methyliodobenzene and Phenylboronic acid; Solvent: H_2O: Ethanol (1:1); Temperature: 80 °C; Time:0.5 h; Conversion: 94%			
29	Pd-Ni/iron oxide core-shell nanoalloys (0.0026 mol% of Pd)	Starting materials: Bromobenzene and Phenylboronic acid; Solvent: Ethanol; Temperature: 80 °C; Time: 30 min; Conversion: 93%	TON: 36538	6	(Ghanbari et al., 2017)
		Starting materials: Iodobenzene and Phenylboronic acid; Solvent: Ethanol; Temperature: 80 °C; Time: 10 min; Conversion: 97%	TON: 37307		

		Starting materials: Chlorobenzene and Phenylboronic acid; Solvent: Ethanol; Temperature: 80 ℃; Time: 60 min; Conversion: 83%	TON: 31923		
30	Bimetallic Ni-Pd Alloy Nanoparticle (0.02 mmol)	Starting materials: Bromobenzene (1 mmol) and Phenylboronic acid (1.2 mmol); Solvent: H_2O: Ethanol (1: 1); Temperature: 50 ℃; Time: 7 h; Conversion: 65%	-	5	(Rai et al., 2015)
		Starting materials: Iodobenzene and Phenylboronic acid; Solvent: H_2O: Ethanol (1: 1); Temperature: 50 ℃; Time: 6 h; Conversion: 90%			
31	Monodispersed Pd-Ni Nanoparticles (0.02 mmol Pd)	Starting materials: 4-bromoanisole (1mmol), phenylboronic acid (2 mmol); Solvent: 1-4 Dioxane; Temperature: 100 ℃; Time: 12 h; Conversion:92%	-	5	(Wu et al., 2011)
32	Ni-Pd bimetallic nanoparticle catalysts	Starting materials: 4-bromoanisole (1.0 mmol), 4-fluoroboronic acid (1.2 mmol): Solvent: $H_2O-C_2H_5OH$ (1:1 v/v, 20 mL): Temperature: 50 ℃; Time: 1 h; Conversion: 74%	TON: 3600	7	(Rai et al., 2016)
33	Palladium and Nickel β-Diimine Complexes (3 mol%)	Starting materials: p-Bromo toluene (1 mmol), and Phenylboronic acid (1. mmol); Solvent: Dioxane; Temperature: 80 ℃; Time: 3h; Conversion: 89%	-	-	(Domin et al., 2005)
34	Core-shell-like Ni-Pd nanoparticles supported on carbon black (5.5 mg, 0.1 mol% Pd)	Starting materials: bromobenzene (2.5 mmol), phenylboric acid (2.75 mmol); Solvent: EtOH/H_2O = 20 mL/20 mL; Temperature: 30 ℃; Time: 1h; Conversion: 91%	-	5	(Xia et al., 2017)
		Starting materials: Iodobenzene (2.5 mmol), phenylboric acid (2.75 mmol); Solvent: EtOH/H_2O = 20 mL/20 mL; Temperature: 30 ℃; Time: 0.5h; Conversion: 90%			
		Starting materials: Chlorobenzene (2.5 mmol), phenylboric acid (2.75 mmol); Solvent: EtOH/H_2O = 20 mL/20 mL; Temperature: 30 ℃; Time: 3h; Conversion: 5%			
35	Pd-Ni nanoparticles supported on titanium oxide (0.002 mmol Pd)	Starting materials: Iodobenzene (0.2 mmol), phenylboric acid (0.3 mmol); Solvent: EtOH/H_2O = 1 mL/1 mL; Temperature: 50 ℃; Time: 5 h; Conversion: 99%	-	4	(Han et al., 2018)
		Starting materials: Bromobenzene (0.2 mmol), phenylboric acid (0.3 mmol); Solvent: EtOH/H_2O = 1 mL/1 mL; Temperature: 50 ℃; Time: 5 h; Conversion: 91%			
		Starting materials: Chlorobenzene (0.2 mmol), phenylboric acid (0.3 mmol); Solvent: EtOH/H_2O = 1 mL/1 mL; Temperature: 50 ℃; Time: 5 h; Conversion: 11%			

36	Pd–Ni bimetal/carbon nanofiber composite catalyst ((5 mg)	Starting materials: Iodobenzene (1 mmol), phenylboric acid (1.1 mmol); Solvent: DMF = 1 mL/1 mL; Temperature: 80 °C; Time: 1 h; Conversion:98.29%	TON: 786 TOF: 786	10	(Bao et al., 2019)
		Starting materials: Bromobenzene (1 mmol), phenylboric acid (1.1 mmol); Solvent: DMF = 1 mL/1 mL; Temperature: 80 °C; Time: 3 h; Conversion:96.5%	TON: 772 TOF: 257		
		Starting materials: Chlorobenzene (1 mmol), phenylboric acid (1.1 mmol); Solvent: DMF = 1 mL/1 mL; Temperature: 80 °C; Time: 5 h; Conversion:7%	-		
37	Palladium grafted on SmDNA supported on silane functionalize magnetite (0.02 mol% Pd)	Starting materials: Bromobenzene (1 mmol), phenylboric acid (1.1 mmol); Solvent: DMF = 1 mL/1 mL; Temperature: 80 °C; Time: 3 h; Conversion:96.5%	TON: 24018 TOF: 96074	6	(Kandathil et al., 2020)
		Starting materials: Chlorobenzene (1 mmol), phenylboric acid (1.1 mmol); Solvent: DMF = 1 mL/1 mL; Temperature: 80 °C; Time: 5 h; Conversion:7%	TON: 22970 TOF: 22970		
38	Pd/DNA C1: 50 mg of fish sperm DNA + Pd target loading: 3.56 mmol/g C2: 50 mg of fish sperm DNA + Pd target loading: 3.61 mmol/g C3: 50 mg of fish sperm DNA + Pd target loading: 2.98 mmol/g C4: 50 mg of fish sperm DNA + Pd target loading: 3.52 mmol/g	Starting materials: 2-Methyl Bromobenzene (1 mmol), phenylboronic acid (1.2 mmol); Solvent: dioxane/water (1:1); Temperature: 80 ◦C; Time: 4 h 73% conversion (With catalyst C1); 75% conversion (With catalyst C2); 64% conversion (With catalyst C3); 59% conversion (With catalyst C4)	-	7	(Mart et al., 2018)
		Starting materials: 4-Methyl Bromobenzene (1 mmol), phenylboronic acid (1.2 mmol); Solvent: dioxane/water (1:1); Temperature: 80 ◦C; Time: 4 h 85% conversion (With catalyst C1); 75% conversion (With catalyst C2); 70% conversion (With catalyst C3); 54% conversion (With catalyst C4)			
39	Calf thymus DNA (ctDNA)-Modified Graphene/Pd Nanoparticles (1.1 mol %)	Starting materials: Iodobenzene (1 mmol), Phenyl Boronic Acid (1.2 mmol): solvent: water with SDS; Temperature: 100; Time: 1.5 h 100% conversion	-	7	(Qu et al., 2012)
40	Pd and Fe_3O_4 functionalized DNA (Sodium salt of salmon milt DNA)	Starting materials: p-Bromo Benzaldehyde (0.95 mmol), Phenyl Boronic Acid (1.05 mmol): solvent: DES; Temperature: 90°C; Time: 2 h	-	6	(Chakraborty et al., 2019)

	(9.4 mol% Pd)	100% conversion, 91.3% selectivity			

7.3. Application of Nanosystems under study for p-nitrophenol reduction reaction

A summary of the efficacy parameters for the various catalyst systems under study are shown in figure 7.3. The recyclability was high for Pd@IO-DTPA-DNA, Pd@Ni@IO-Chitosan and Pd@Ni@IO-DTPA while the rate constant was highest for Pd@Ni@IO-Chitosan.

The rate constants were much better than literature reported catalyst systems except for Pd/TiO_2 (Table 7.3, entry 9); Pd/PdO nanoparticles supported on oxidized multi-walled carbon nanotubes (Table 7.3, entry 12) and palladium nanocubes (Table 7.3, entry 13)

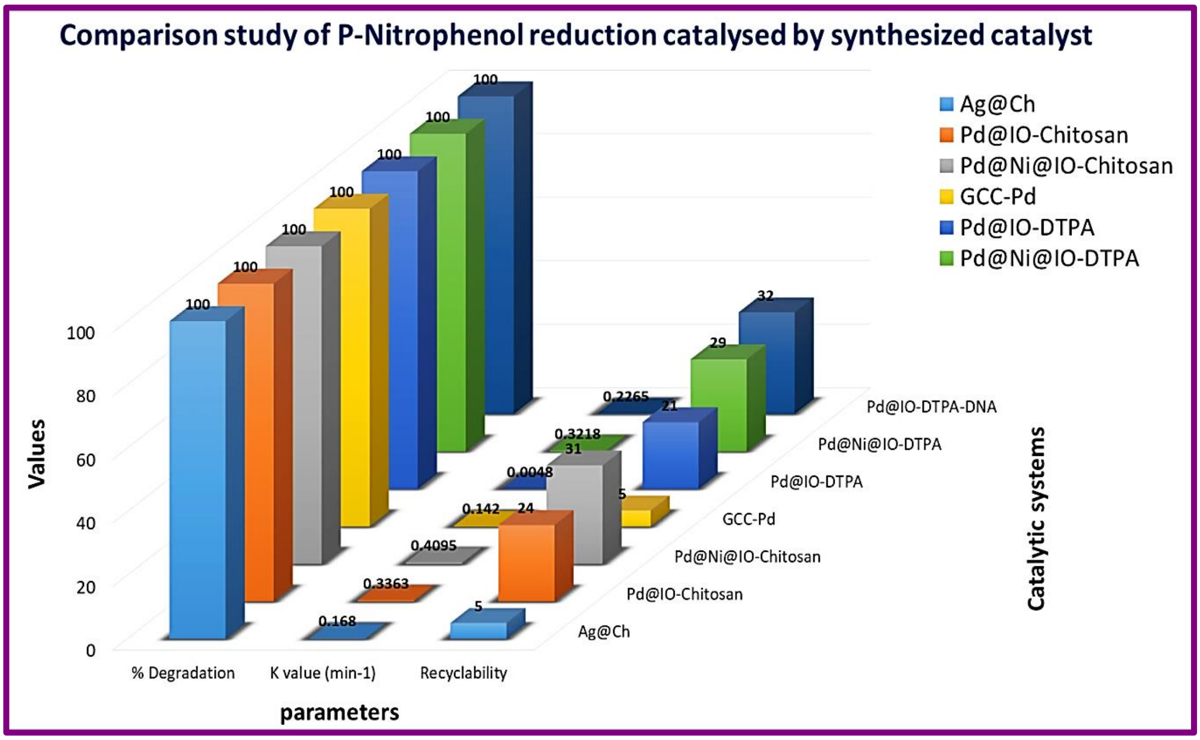

Figure 7.3: Comparison Study of p-Nitrophenol reduction catalysed by Synthesized catalyst, Reaction conditions: for Pd@IO-Chitosan, Pd@Ni@IO-Chitosan, Pd@IO-DTPA, Pd@Ni@IO-DTPA: 25 ppm 50 mL p-NP, $NaBH_4$: 7-12 mg, Time: 8-12 min, catalyst 1 mg; For Ag@Ch: 10 ppm 10 mL p-NP; $NaBH_4$: 2 mg, Time: 15 min, catalyst: 1 mg; For Pd@GCC: 10 ppm 10 mL p-NP; $NaBH_4$: 4mg, Time: 25 min, catalyst: 1 mg

7.3.1. The plausible mechanism of the reduction of the p-NP by Pd/Ag nanoparticles

The kinetics of this model reaction was explained using the Langmuir-Hinshelwood (LH) model, according to Ballauff and his team (Zhao et al., 2015). (Figure 7.4)

Firstly, both the reactants adsorb on the surface of the catalyst. Both substrates adsorb quickly and the process is treated as an equilibrium process. The reduction of p-NP, which is the rate-determining step is provoked by the interaction of the adsorbed p-NP with hydrogen atoms bound on the active surfaces of NPs. As a result of reduction reaction, p-AP is formed followed by the desorption of product from the metal surfaces and reactivation of the catalytic system. The borohydride ion transfers hydrogen on the surface in a reversible manner and the nitrophenol is reduced.

The rate determining step consists of the reduction of nitrophenol by the surface hydrogen species. The reaction rate can therefore be related to the total surface of the nanoparticles, the kinetic constant K related to the rate-determining step, and the adsorption constants K_{NP} and K_{BH4} of nitrophenol and borohydride respectively (Aditya et al., 2015; Veerakumar et al., 2014).

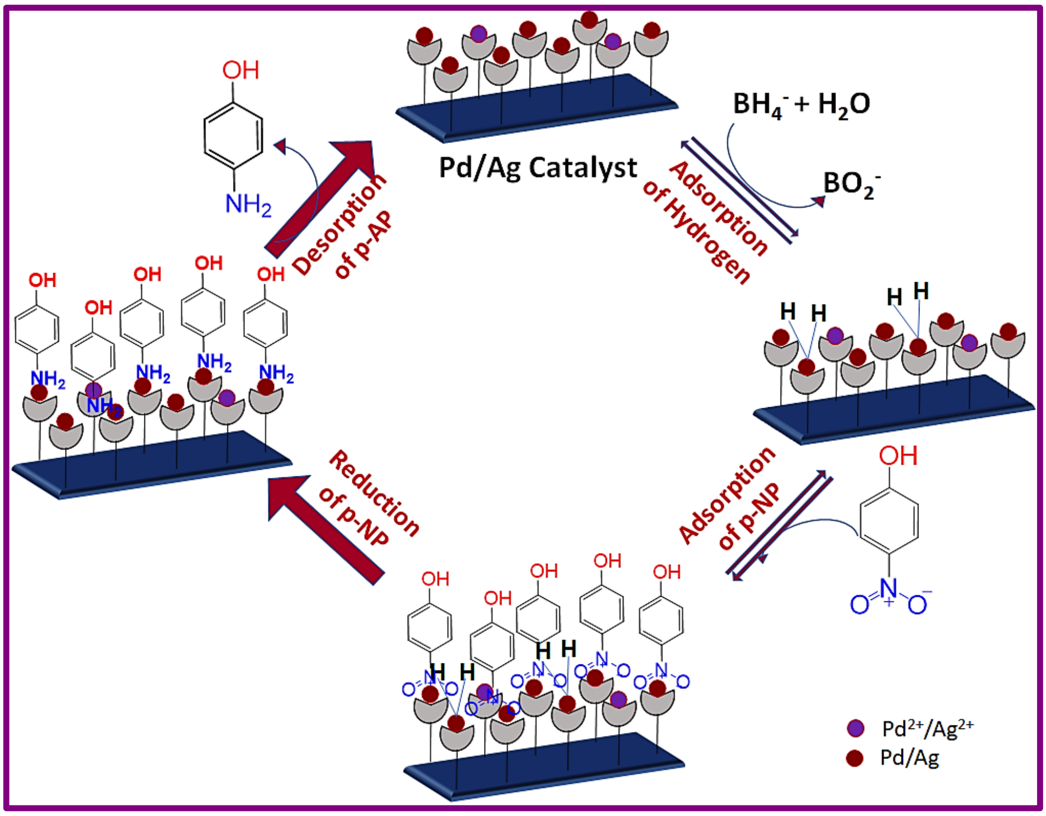

Figure 7.4: *Plausible mechanism from p-Nitrophenol reduction reaction*

Reduction performed with Ni@IO-DTPA gave 5.998% conversion. Therefore, a **synergistic catalytic probable mechanism** (Figure 7.5) has been proposed for Pd@Ni@IO-DTPA to elucidate the catalytic activity of Pd@Ni@IO-DTPA. According to Langmuir–Hinshelwood mechanism, the p-NP reduction by BH_4^- is governed by the efficient adsorption of both reactants and rapid hydrogen transfer from BH_4^- to p-NP over metal catalysts. As discussed in chapter 3 and in table 7.1, the catalyst Pd@Ni@IO-DTPA contain Pd, PdO, Ni and $Ni(OH)_2$

which gives electron deficient and electrophilic catalytic surface. p-NP molecules deprotonate in the presence of BH_4^- and form 4-nitrophenolate ions. p-Nitrophenolate and BH_4^- ions are negatively charged and preferentially adsorbed by the electrophilic Pd@Ni nanocatalyst. The BH_4^- ions donate electrons to the electron-deficient Pd@Ni nanocatalyst and generate active hydrogen atoms through the cleavage of B-H bond over Pd@Ni nanocatalyst. The active hydrogen atoms are thermodynamically unstable and readily react with p-nitrophenolate ions through a conventional hydrogenation route. In the last step, p-aminophenol formed and detached from the metal surface, thus creating a free surface and the catalytic cycle starts again (Liu et al., 2016).

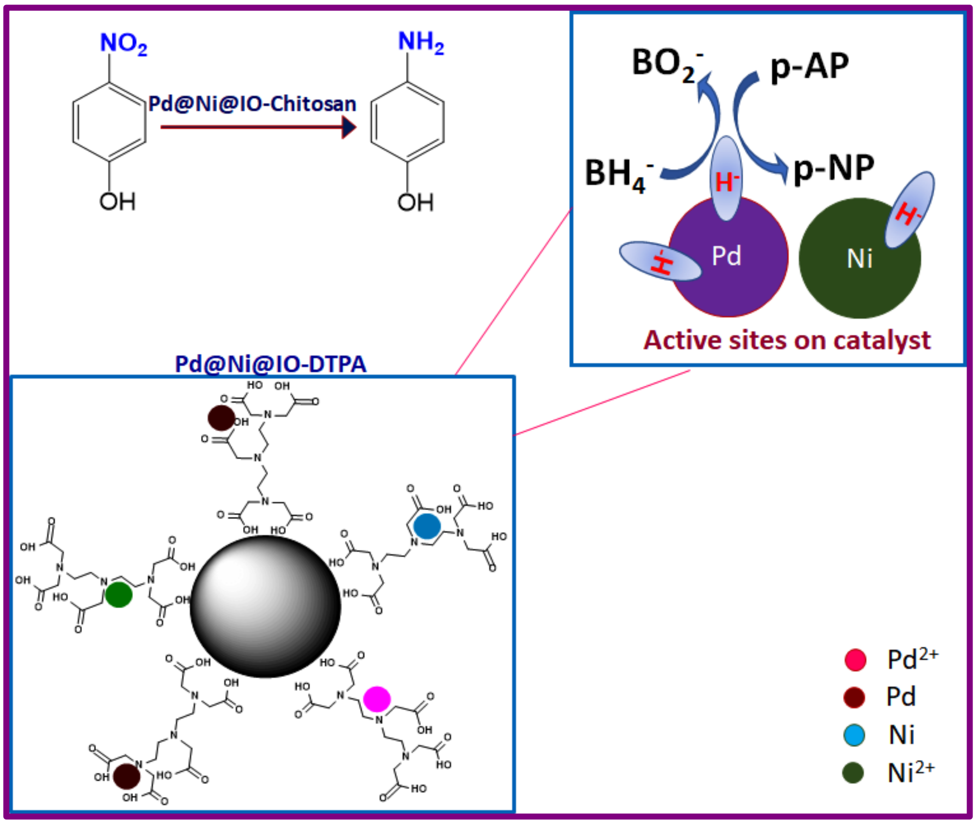

Figure 7.5: *probable mechanism p-NP reduction reaction catalysed by Pd@Ni@IO-DTPA*

Table 7.3: Comparative study with literature reported catalysts for p-NP reduction

Sr. No.	Catalyst	Reaction condition	K Value	Recyclability	Ref.
1	Pd deposited on SBA-15; Pd/SBA-15	Reagents: Pd: PNP: $NaBH_4$ molar ratio of 1: 10: 1000; Time: 15 min	$7.15X10^{-1}$ s^{-1}	-	(El-Sheikh et al., 2013)
2	Palladium supported Thiol Functionalized Cross-Linked Chitosan; Pd/CS-TPA-SH (0.02 g)	Reagents: 3 mL 0.17 mM PNP, 0.25mL 0.5 M $NaBH_4$; Time: 60 Sec		2	(Zhang et al., 2017)
3	Chitosan supported palladium nanoparticles Chitosan/Pd (0.5 mg)	Reagents: 400µl, 10^{-4} M PNP, 400µl, 1.5 mmol $NaBH_4$ Time: CS/Pd-5%: 36 min; CS/Pd-10%: 22 min; CS/Pd-15%: 18 min	CS/Pd-5%: 1.95×10^{-3} s^{-1}, CS/Pd-10%: 2.41×10^{-3} s^{-1}, CS/Pd-15%: 4.01×10^{-3} s^{-1}	-	(Dhanavel et al., 2018)
4	palladium-nickel/iron oxide core-shell nanoalloy; 1.03 µg Pd	Reagents: 1.7 ml, 0.2 mM p-NP; 0.7 mL, 15Mm $NaBH_4$; Time: 11.6 min	-	6	(Ghanbari et al., 2017)
5	graphene-supported palladium-nickel alloy nanoparticles	Reagents: 2.8 ml, 0.5 Mm p-NP; 400 µl, 0.3 mM $NaBH_4$; Time: 12 min		3	(Revathy et al., 2018)
6	Nanostructured Pd-Sch-δ-FeOOH particles	Reagents: 1 ml 1.25×10^{-4} M p-NP, 0.1 ml $NaBH_4$ (0.05 M) Catalyst: 10 mg; Time: 2 min	$0.012 s^{-1}$	6	(Çalıs et al., 2021)
7	Palladium on melamine functionalized magnetic chitosan beads (Fe_3O_4/CS-Me@Pd)	Reagents: 5 mL of p-NP (1 mg/ mL) solution, $NaBH_4$ solution (1 mg/mL) Catalyst: 6.0, 8.0, 10.0, 12.0 mg ; Time: 5 min	0.0165 s^{-1}	6	(G. Wang et al., 2021)
8	PVA-Stabilized Palladium nanoparticles	Reagents: 0.133 mM p-NP, 3.33 mM $NaBH_4$; Catalyst: 22 µL; Time: 9 min	*0.035* s^{-1}	3	(Chatterjee & Bhattacharya, 2021)
9	Pd/TiO_2	Reagents: 2.7 ml 0.18 mM p-NP, 0.3 mL $NaBH_4$; Catalyst: 0.2 wt%; Time: 5 min	0.632 min^{-1}	5	(Rogers et al., 2018)

10	Oxygen deficient Pr_6O_{11} nanorod supported palladium nanoparticles	Reagents: (100 mL, 10 mM) 4-nitrophenol, (8 mL, 0.1 M) $NaBH_4$ Catalyst: 100 mL, 1.4 mg mL^{-1}; Time: 3 min	0.0191 s^{-1}	10	(Jiang et al., 2018)
11	Double-shelled hollow nanospheres (HNSs) supported Pd nanoparticles; Fe@NC@Pd	Reagents: 3 ml 10 mM 4-nitrophenol, 13.4 mg $NaBH_4$; Catalyst: 2 mg; Time: 18 min	-	9	(Duan et al., 2018)
12	Pd/PdO nanoparticles supported on oxidized multi-walled carbon nanotubes; (2 mmol%)	Reagents: 1.5 ml 0.1 mM 4-nitrophenol, 1.5 ml 10 mM $NaBH_4$ Catalyst: 34 µL; Time: Pd-n catalysts: Pd-1: 240sec, Pd-2: 420 sec, Pd-3: 480 sec, Pd-4: 900 sec	Pd-1: 0.6 min^{-1}; Pd-2: 0.25 min^{-1}, ; Pd-3: 0.15 min^{-1}; Pd-4: 0.1 min^{-1}	10	(C. Wang et al., 2015)
13	Palladium nanocubes (2 mg)	Reagents: 20 µL (0.01 M) p-NP, 10 µL (0.5 M) $NaBH_4$; Catalyst: 70 µL; Time: 6 min	7.3×10^{-1} min^{-1}	6	(Swain et al., 2020b)
14	Ni-Pd nanodimers on nitrogen-doped reduced graphene oxide	Reagents: 125 µL (0.05 M) p-NP, 125 µL (0.1 M) $NaBH_4$; Catalyst: 2 mg mL^{-1}; Time: 160 sec	0.0170 s^{-1}	10	(Liu et al., 2016)
15	Pd−DNA−Fe_3O_4 (180 mg; 3.3 mol% Pd)	Reagents: 1.0 mmol (0.123g) nitrobenzene; 10.0 mmol (0.625g) hydrazine hydrate; Time: 6h; Temperature: 85 °C		6	(Chakraborty et al., 2019)
16	DNA metallization with Pd	Reagents: 0.02 mM p-nitrophenol; 10 mM $NaBH_4$; Time: 5 min;		-	(Zinchenko et al., 2016)
17	Pd−protein nanocomposites	Reagents: 0.22 mM 197 µL p-nitrophenol; 33.33 mM $NaBH_4$; Catalyst: 3 µL; Time: 30 min		5	(Yu et al., 2020)
18	Silver nanoparticles deposited on magnetic chitosan (Fe_3O_4@CS@MS@Ag)	Reagents: 6.0 mL, 10.0 mg /L p-nitrophenol; 1.0 mL, 1.0 mM $NaBH_4$; Catalyst: 1.5 mg/0.8 mg; time: 10 min: 90% conversion	-	5	(Hasan et al., 2019)
19	silver (Ag) nanoparticles deposited on magnetic chitosan (CS) microcapsules; Fe_3O_4/CS-Ag	Reagents: 6.0 mL, (10-40 mg /L) p-nitrophenol; 2 mL of 0.5 mM $NaBH_4$; Catalyst: 1 mg; time: 15 min: 98% conversion	-	10	(Xu et al., 2017)
20	Pd supported on Chitosan-carbon nanotube	Reagents: (1.0 mL, 1.0×10^{-4} M) p-nitrophenol; 0.1 mL, 0.05 M $NaBH_4$; Catalyst: 4 mg; time: 12 min: 98% conversion	-	6	(Sargin et al., 2020)

7.4. Application of Nanosystems under study for Dye degradation

Metal nanoparticles such as palladium is needed to reduce the dye completely to the degradation product. Firstly, $NaBH_4$ is decomposed into BH_4^- by Pd NPs and produces H–Pd and Pd-BH_3^- as reactive intermediates. BH_4^- ions are nucleophilic, while dyes (MG, MB, R6G, CV) are electrophilic with respect to Pd NPs, where the Palladium accept electrons from BH_4^- and transfer them to the dye molecule. Here, the Pd–H reagent is responsible intermediate to convert the toxic dye molecule into a harmless degradation product for all dye molecules. (Ganapuram et al., 2015; Sahin & Gubbuk, 2022).

$$2Pd + BH_4^- \leftrightarrow Pd{-}BH_3^- + Pd{-}H$$

$$H{-}Pd + PdNPs \rightarrow Pd{-}Dye + Pd + H$$

$$Pd{-}BH_3^- + PdNPs \rightarrow Pd{-}Dye + Pd + BH_3$$

The comparison of recyclability and K value with literature reported palladium catalysts for dye degradation are tabulated in Table 7.5. Recyclability of the catalyst under study in the present work was better than the reported catalysts.

Table 7.4: Comparative performance with reported Pd catalysts for dye degradation

Entry	Catalyst	Reaction condition	K Value	Recyclability	Ref.
1	Pd nanoparticles decorated on ZSM-5 (0.5 mg)	MB: 2.5 mL of 25 ppm; $NaBH_4$: 200 µL 0.2 M; Time: 12 min	-	6	(Subhan et al., 2021)
2	Pd NPs synthesized using carob, cinnamon, Ginger and turmeric antioxidant extracts	MB: 1 mL (1×10^{-5} mg L^{-1}); $NaBH_4$: 1 mL (1×10^{-2} mol L^{-1}); Time: 20, 15, 17.5, 21 min	0.0699, 0.0912, 0.0820, 0.0651	-	(Sahin & Gubbuk, 2022)
3	Pd supported on chitosan-carbon nanotube (4 mg)	MB: (1.0 mL, 1.0×10^{-4} M); $NaBH_4$: 3 mg; Time: 1 min	-	**6**	(Sargin et al., 2020)
4	Pd supported on Polyaniline	MB: (2.0×10^{-6} M); $NaBH_4$: 5 mg; Time: 8 min	-	**4**	(Roy et al., 2019)
5	Graphene Oxide/Palladium nanocomposite (5 mg)	MB: (25 ml, 10 ppm); $NaBH_4$: 25 ml 5.3×10^{-3} M; Time: 10 sec		5	(Omidvar et al., 2017)
6	Pd@GCC	Dye: (25 ml, 10 ppm); MG: 1 mg $NaBH_4$; Time: 10 sec MB: 3 mg $NaBH_4$; Time:6 min CV: 1 mg $NaBH_4$; Time: 6 min R6G: 2 mg $NaBH_4$; Time: 30 min	MB: 0.80 min^{-1} CV: 0.803 min^{-1} R6g: 0.348 min^{-1}	8	Present work

9.5. Future Scope of the Present work

- The present nanocatalysts were synthesized by self assembly and was not controlled. Controlled synthesis with more Nickel and less palladium has to be attempted and its catalytic activity has to be evaluated from economic point of view
- The scope of the catalyst for more substrates has to be studied to further prove the versatility of the .
- The DNA based catalyst has to be investigated for synthesis of wider range of chiral products
- The DTPA and chitosan-based support systems can be investigated for recovery of Palladium from ELP solutions. Especially the Ni based systems would be very interesting
- Synthesis and study of Pd@Ni@IO-DTPA-DNA may give interesting results.

9.6. References

Abdol R. Hajipour, & Tavangar-Rizi, Z. (2017). Palladium nanoparticles immobilized on magnetic methionine- functionalized chitosan: A versatile catalyst for Suzuki and copper-free Sonogashira reactions of aryl halides at room temperature in water as only solvent. *Appl. Organometal. Chem.*, *31*(9), e3701. https://doi.org/10.1002/aoc.3701

Aditya, T., Pal, A., & Pal, T. (2015). Nitroarene reduction: A trusted model reaction to test nanoparticle catalysts. *Chem. Commun.*, *51*(46), 9410–9431. https://doi.org/10.1039/c5cc01131k

Amirmahani, N., Mahmoodi, N. O., Malakootian, M., Pardakhty, A., & Seyedi, N. (2021). Introduction of PdCl2 supported on tartaric acid modified magnetite nanoparticles (Fe3O4@TA-Pd) as a novel catalytic system in Suzuki–Miyaura coupling reaction. *Materials Chemistry and Physics*, *267*, 124698. https://doi.org/10.1016/j.matchemphys.2021.124698

Anuradha, Shweta Kumari, Layeka, S., & Pathak, D. D. (2017). Palladium nanoparticles immobilized on a magnetic Chitosan-anchored Schiff base: Application in Suzuki-Miyaura and Heck-Mizoroki coupling reactions. *New Journal of Chemistry*, *41*, 5595–5604. https://doi.org/10.1039/C7NJ00283A

Ariannezhad, M., Pourmorteza, N., Yousefi, A., & Esperi, M. (2022). Catalytic reduction of nitroarenes and Suzuki-Miyaura reactions using Pd complex stabilized on the functionalized polymeric support. *Chemical Physics Letters*, *793*, 139431. https://doi.org/10.1016/j.cplett.2022.139431

Bao, G., Bai, J., & Li, C. (2019). Synergistic effect of the Pd–Ni bimetal/carbon nano fiber composite catalyst in Suzuki coupling. *Org. Chem. Front.*, *6*(3), 352–361.

https://doi.org/10.1039/c8qo01100a

Baran, N. Y., Baran, T., & Mente, A. (2018). Production of novel palladium nanocatalyst stabilized with sustainable chitosan/cellulose composite and its catalytic performance in Suzuki- Miyaura coupling reactions. *Carbohydrate Polymers*, *181*, 596–604. https://doi.org/10.1016/j.carbpol.2017.11.107

Baran, T. (2019). Production and Application of Highly Efficient and Reusable Palladium Nanocatalyst Decorated on the Magnetically Retrievable Chitosan/Activated Carbon Composite Microcapsules. *Catalysis Letters*, *149*(6), 1496–1503. https://doi.org/10.1007/s10562-019-02739-1

Baran, T., & Nasrollahzadeh, M. (2019). Facile synthesis of palladium nanoparticles immobilized on magnetic biodegradable microcapsules used as effective and recyclable catalyst in Suzuki-Miyaura reaction and p -nitrophenol reduction. *Carbohydrate Polymers*, *222*, 115029. https://doi.org/10.1016/j.carbpol.2019.115029

Baran, T., Nuray Yılmaz Baran, & Menteş, A. (2017). Sustainable chitosan / starch composite material for stabilization of palladium nanoparticles : Synthesis , characterization and investigation of catalytic behaviour of Pd @ chitosan / starch nanocomposite in Suzuki – Miyaura reaction. *Appl. Organometal. Chem.*, *32*(2), e4075. https://doi.org/10.1002/aoc.4075

Baran, T., Sargin, I., Menteş, A., & Kaya, M. (2016). Exceptionally high turnover frequencies recorded for a new chitosan-based palladium (II) catalyst. *Applied Catalysis A : General*, *523*, 12–20. https://doi.org/10.1016/j.apcata.2016.05.012

Baran, T., & Tulden Inanan Ayfer Mentes. (2016). Synthesis, Characterization, and Catalytic Activity in Suzuki Coupling and Catalase-like Reactions of New Chitosan Supported Pd Catalyst. *Carbohydrate Polymers*, *145*, 20–29. https://doi.org/10.1016/j.carbpol.2016.03.019

Begum, T., Mondal, M., Borpuzari, M. P., Kar, R., Kalita, G., Gogoi, P. K., & Bora, U. (2017). Immobilized symmetrical bis-(NHC) palladium complex as a highly efficient and recyclable Suzuki-Miyaura catalyst in aerobic aqueous media. *Dalton Trans.*, *46*(2), 539–546. https://doi.org/10.1039/C6DT03097A

Çalıs, M., Baran, T., & Nasrollahzadeh, M. (2021). Facile preparation of nanostructured Pd-Sch- δ -FeOOH particles : A highly effective and easily retrievable catalyst for aryl halide cyanation and p -nitrophenol reduction. *Journal of Physics and Chemistry of Solids*, *152*, 109968. https://doi.org/10.1016/j.jpcs.2021.109968

Chakraborty, S., Mruthunjayappa, M. H., Aruchamy, K., Singh, N., Prasad, K., Kalpana, D., Ghosh, D., Kotrappanavar, N. S., & Mondal, D. (2019). Facile Process for Metallizing DNA in a Multitasking Deep Eutectic Solvent for Ecofriendly C–C Coupling Reaction and Nitrobenzene Reduction [Research-article]. *ACS Sustainable Chemistry & Engineering*, *7*, 14225–14235. https://doi.org/10.1021/acssuschemeng.9b03224

Chatterjee, S., & Bhattacharya, S. K. (2021). Size-Dependent Catalytic Activity of PVA-Stabilized Palladium Nanoparticles in p - Nitrophenol Reduction: Using a

Thermoresponsive Nanoreactor. *ACS Omega*, *6*(32), 20746−20757. https://doi.org/10.1021/acsomega.1c00896

Chen, J., Vasiliev, A. N., Panarello, A. P., & Khinast, J. G. (2007). Pd-leaching and Pd-removal in Pd/C-catalyzed Suzuki couplings. *Applied Catalysis A*, *325*, 76–86. https://doi.org/10.1016/j.apcata.2007.03.010

Dehghani, M., Tadjarodi, A., & Chamani, S. (2019). Synthesis and Characterization of Magnetic Zeolite Y−Palladium−Nickel Ferrite by Ultrasonic Irradiation and Investigating Its Catalytic Activity in Suzuki − Miyaura Cross-Coupling Reactions [Research-article]. *ACS Omega*, *4*, 10640–10648. https://doi.org/10.1021/acsomega.9b00666

Dhanavel, S., Manivannan, N., Mathivanan, N., Gupta, V. K., Narayanan, V., & Stephen, A. (2018). Preparation and characterization of cross-linked chitosan/palladium nanocomposites for catalytic and antibacterial activity. *Journal of Molecular Liquids*, *257*(B), 32–41. https://doi.org/10.1016/j.molliq.2018.02.076

Domin, D., Benito-garagorri, D., Mereiter, K., Frohlich, J., & Kirchner, K. (2005). Synthesis and Reactivity of Palladium and Nickel -Diimine Complexes : Application as Catalysts for Heck , Suzuki , and Hiyama Coupling Reactions †. *Organometallics*, *24*, 3957–3965. https://doi.org/10.1021/om050201h

Dong, Y., Bi, J., Ming, S., Zhang, S., Zhu, D., Meng, D., & Li, T. (2021). Functionalized chitosan as a novel support for stabilizing palladium in Suzuki reactions. *Carbohydrate Polymers*, *260*, 117815. https://doi.org/10.1016/j.carbpol.2021.117815

Duan, X., Liu, J., Hao, J., Wu, L., He, B., Qiu, Y., Zhang, J., He, Z., Xi, J., & Wang, S. (2018). Magnetically recyclable nanocatalyst with synergetic catalytic effect and its application for 4-nitrophenol reduction and Suzuki coupling reactions. *Carbon*, *130*, 806–813. https://doi.org/10.1016/j.carbon.2018.01.038

El-Sheikh, S. M., Ismail, A. A., & Al-Sharab, J. F. (2013). Catalytic reduction of p-nitrophenol over precious metals/highly ordered mesoporous silica. *New Journal of Chemistry*, *37*, 2399–2407. https://doi.org/10.1039/c3nj00138e

Fakhri, A., & Naghipour, A. (2017). chitosan-pd (ii) complex-decorated fe3o4 nanoparticle as the highly effective and magnetically recyclable catalyst for suzuki and heck coupling reactions. *Comments on Inorganic Chemistry*, *37*(4), 201–218. https://doi.org/10.1080/02603594.2017.1282351

Ganapuram, B. R., Alle, M., Dadigala, R., Dasari, A., Maragoni, V., & Guttena, V. (2015). Catalytic reduction of methylene blue and Congo red dyes using green synthesized gold nanoparticles capped by salmalia malabarica gum. *International Nano Letters*, *5*, 215–222. https://doi.org/10.1007/s40089-015-0158-3

Gautam, P., & Bhanage, B. M. (2015). Palladacycle Catalyzed Carbonylative Suzuki – Miyaura Coupling with High Turnover Number and Turnover Frequency. *J. Org. Chem.*, *80*(15), 7810–7815. https://doi.org/10.1021/acs.joc.5b01160

Ghanbari, N., Hoseini, S. J., & Bahrami, M. (2017). Ultrasonic assisted synthesis of palladium-nickel/iron oxide core-shell nanoalloys as effective catalyst for Suzuki-Miyaura and p -nitrophenol reduction reactions. *Ultrasonics - Sonochemistry*, *39*, 467–477. https://doi.org/10.1016/j.ultsonch.2017.05.015

Hajipour, A. R., Sadeghi, A. R., & Khorsandi, Z. (2017). Pd nanoparticles immobilized on magnetic chitosan as a novel reusable catalyst for green Heck and Suzuki cross-coupling reaction: In water at room temperature. *Applied Organometallic Chemistry*, *32*(3), e4112. https://doi.org/10.1002/aoc.4112

Han, D., Zhang, Z., Bao, Z., Xing, H., & Ren, Q. (2018). Pd-Ni nanoparticles supported on titanium oxide as effective catalysts for Suzuki-Miyaura coupling reactions. *Front. Chem. Sci. Eng.*, *12*(1), 24–31. https://doi.org/10.1007/s11705-017-1669-4

Hasan, K. (2020). Methyl Salicylate Functionalized Magnetic Chitosan Immobilized Palladium Nanoparticles: An Efficient Catalyst for the Suzuki and Heck Coupling Reactions in Water. *ChemistrySelect*, *5*(23), 7129–7140. https://doi.org/10.1002/slct.202001933

Hasan, K., Shehadi, I. A., Al-bab, N. D., & Elgamouz, A. (2019). Magnetic Chitosan-Supported Silver Nanoparticles : *Catalysts*, *9*(10), 839. https://doi.org/10.3390/catal9100839

Jiang, N., Zhou, X., Jiang, Y.-F., Zhao, Z.-W., Ma, L.-B., Shen, C.-C., Liu, Y.-N., Yuan, C.-Z., Sahar, S., & Xu, A.-W. (2018). Oxygen deficient Pr6O11 nanorod supported palladium nanoparticles: highly active nanocatalysts for styrene and 4-nitrophenol hydrogenation reactions. *RSC Adv.*, *8*, 17504–17510. https://doi.org/10.1039/c8ra02831a

Kandathil, V., Kempasiddaiah, M., Nataraj, S. K., Somappa, S. B., & Patil, S. A. (2020). DNA as a bioligand supported on magnetite for grafting palladium nanoparticles for cross-coupling reaction. *Appl. Organometal. Chem.*, *34*(3), e5357. https://doi.org/10.1002/aoc.5357

Liu, L., Chen, R., Liu, W., Wu, J., & Gao, D. (2016). Catalytic reduction of 4-nitrophenol over Ni-Pd nanodimers supported on nitrogen-doped reduced graphene oxide. *Journal of Hazardous Materials*, *320*, 96–104. https://doi.org/10.1016/j.jhazmat.2016.08.019

Mart, M., Tylus, W., & Trzeciak, A. M. (2018). Pd/DNA as Highly Active and Recyclable Catalyst of Suzuki–Miyaura Coupling. *Catalysts*, *8*(11), 552. https://doi.org/10.3390/catal8110552

Melike Çalışkan, & Baran, T. (2021). Decorated palladium nanoparticles on chitosan/δ-FeOOH microspheres: A highly active and recyclable catalyst for Suzuki coupling reaction and cyanation of aryl halides. *International Journal of Biological Macromolecules*, *174*, 120–133. https://doi.org/10.1016/j.ijbiomac.2021.01.162

Molaei, S., & Ghadermazi, M. (2021). Anchoring of palladium onto the surface of porous MCM-41 modified with DL-pyroglutamic acid as a novel heterogeneous catalyst for Suzuki – Miyaura coupling reactions. *Journal of Organometallic Chemistry*, *953*, 122064. https://doi.org/10.1016/j.jorganchem.2021.122064

Naghipour, A., & Fakhri, A. (2016). Heterogeneous Fe3O4@chitosan-Schiff base Pd nanocatalyst: Fabrication, characterization and application as highly efficient and magnetically-recoverable catalyst for Suzuki-Miyaura and Heck-Mizoroki C-C coupling reactions. *Catalysis Communications*, *73*, 39–45. https://doi.org/10.1016/j.catcom.2015.10.002

Omidvar, A., Jaleh, B., & Nasrollahzadeh, M. (2017). Preparation of the GO/Pd nanocomposite and its application for the degradation of organic dyes in water. *Journal of Colloid and Interface Science*, *496*, 44–50. https://doi.org/10.1016/j.jcis.2017.01.113

Online, V. A., Tao, S., Yu, Y., Du, X., & Wang, S. (2016). Preparing Magnetic Multicomponent Catalysts via the Bio- inspired Assembly For Heterogeneous Reactions. *RSC Adv.*, *6*, 69909–69918. https://doi.org/10.1039/C6RA12088A

Qu, K., Wu, L., Ren, J., & Qu, X. (2012). Natural DNA-Modified Graphene/Pd Nanoparticles as Highly Active Catalyst for Formic Acid Electro-Oxidation and for the Suzuki Reaction. *ACS Applied Materials and Interfaces*, *4*, 5001–5009. https://doi.org/10.1021/am301376m

Rai, R. K., Gupta, K., Behrens, S., Li, J., Xu, Q., & Singh, S. K. (2015). Highly Active Bimetallic Nickel – Palladium Alloy Nanoparticle Catalyzed Suzuki – Miyaura Reactions. *ChemCatChem*, *7*, 1806–1812. https://doi.org/10.1002/cctc.201500145

Rai, R. K., Gupta, K., Tyagi, D., Mahata, A., Behrens, S., Yang, X., Xu, Q., Pathak, B., & Singh, S. K. (2016). Access to highly active Ni-Pd bimetallic nanoparticle catalysts for C-C coupling reactions. *Catalysis Science and Technology*, *6*(14), 5567–5579. https://doi.org/10.1039/c6cy00037a

Revathy, T. A., Dhanavel, S., Sivaranjani, T., Narayanan, V., Maiyalagan, T., & Stephen, A. (2018). Highly active graphene-supported palladium-nickel alloy nanoparticles for catalytic reduction of 4-nitrophenol. *Applied Surface Science*, *449*, 764–771. https://doi.org/10.1016/j.apsusc.2018.01.280

Rogers, S. M., Richard, C., Catlow, A., Gianolio, D., Wells, P. P., & Dimitratos, N. (2018). Supported metal nanoparticles with tailored catalytic properties through sol-immobilisation: applications for the hydrogenation of nitrophenols. *Faraday Discussions*, *208*, 443–454. https://doi.org/10.1039/c7fd00216e

Roy, M., Mondal, A., Mondal, A., Das, A., & Mukherjee, D. (2019). Polyaniline Supported Palladium Catalyzed Reductive Degradation of Dyes Under Mild Condition. *Current Green Chemistry*, *6*(7), 69–75. https://doi.org/10.2174/2213346106666190130101109

Sahin, M., & Gubbuk, I. H. (2022). Green synthesis of palladium nanoparticles and investigation of their catalytic activity for methylene blue, methyl orange and rhodamine B degradation by sodium borohydride. *Reaction Kinetics, Mechanisms and Catalysis*, *135*, 999–1010. https://doi.org/10.1007/s11144-022-02185-y

Sargin, I., Baran, T., & Arslan, G. (2020). Separation and Purification Technology Environmental remediation by chitosan-carbon nanotube supported palladium nanoparticles : Conversion of toxic nitroarenes into aromatic amines , degradation of dye pollutants and green synthesis of biaryls. *Separation and Purification Technology*, *247*, 116987. https://doi.org/10.1016/j.seppur.2020.116987

Sedghi, R., Heidari, B., Shahmohamadi, H., Zarshenas, P., & Varma, R. S. (2019). Pd nanocatalyst adorned on magnetic chitosan@N-Heterocyclic carbene: Eco-compatible suzuki cross-coupling reaction. *Molecules*, *24*(17), 3048. https://doi.org/10.3390/molecules24173048

Shahbazi, E., & Bahrami, K. (2020). Palladium Nanoparticles Doped on the Chitosan Nanofibers Modified with 2-Aminobenzaldehyde as a Nanocatalyst in Cross-Coupling Reactions. *ChemistrySelect*, *5*, 5489–5496. https://doi.org/10.1002/slct.202000754

Sin, E., Yi, S. S., & Lee, Y. S. (2010). Chitosan-g-mPEG-supported palladium (0) catalyst for Suzuki cross-coupling reaction in water. *Journal of Molecular Catalysis A: Chemical*, *315*(1), 99–104. https://doi.org/10.1016/j.molcata.2009.09.007

Subhan, F., Aslam, S., Yan, Z., & Yaseen, M. (2021). Journal of Environmental Chemical Engineering Palladium nanoparticles decorated on ZSM-5 derived micro- / mesostructures (MMZ) for nitrophenol reduction and MB degradation in water. *Journal of Environmental Chemical Engineering*, *9*(1), 105002. https://doi.org/10.1016/j.jece.2020.105002

Swain, S., Bhavya, M. B., Kandathil, V., Bhol, P., Samal, A. K., & Patil, S. A. (2020a). Controlled Synthesis of Palladium Nanocubes as an Efficient Nanocatalyst for Suzuki−Miyaura Cross-Coupling and Reduction of p-Nitrophenol. *Langmuir*, *36*, 5208–5218. https://doi.org/10.1021/acs.langmuir.0c00526

Swain, S., Bhavya, M. B., Kandathil, V., Bhol, P., Samal, A. K., & Patil, S. A. (2020b). Controlled Synthesis of Palladium Nanocubes as an Efficient Nanocatalyst for Suzuki−Miyaura Cross-Coupling and Reduction of p-Nitrophenol. *Langmuir*, *36*(19), 5208–5218. https://doi.org/10.1021/acs.langmuir.0c00526

Veerakumar, P., Madhu, R., Chen, S., Veeramani, V., Hung, C., Tang, P., Wang, C., & Liu, S. (2014). Highly stable and active palladium nanoparticles supported on porous carbon for practical catalytic applications. *Journal of Materials Chemistry A*, *2*, 16015–16022. https://doi.org/10.1039/C4TA03097D

Veisi, H., Najafi, S., & Hemmati, S. (2018). Pd(II)/Pd(0) anchored to magnetic nanoparticles (Fe3O4) modified with biguanidine-chitosan polymer as a novel nanocatalyst for Suzuki-Miyaura coupling reactions. *International Journal of Biological Macromolecules*, *113*(1), 186–194. https://doi.org/10.1016/j.ijbiomac.2018.02.120

Veisi, H., Ozturk, T., Karmakar, B., Tamoradi, T., & Hemmati, S. (2020). In situ decorated Pd NPs on chitosan-encapsulated Fe3O4/ SiO2 -NH2 as magnetic catalyst in Suzuki-Miyaura coupling and 4-nitrophenol reduction. *Carbohydrate Polymers*, *235*, 115966. https://doi.org/10.1016/j.carbpol.2020.115966

Vibhute, S. P., Mhaldar, P. M., Shejwal, R. V, & Pore, D. M. (2020). Magnetic nanoparticles-supported palladium catalyzed Suzuki-Miyaura cross coupling. *Tetrahedron Letters*, *61*(11), 151594. https://doi.org/10.1016/j.tetlet.2020.151594

Wang, C., Yang, F., Yang, W., Ren, L., Zhang, Y., Jia, X., Zhang, L., & Li, Y. (2015). PdO nanoparticles enhancing the catalytic activity of Pd/carbon nanotubes for 4-nitrophenol reduction. *RSC Advances*, *5*(35), 27526–27532. https://doi.org/10.1039/C4RA16792A

Wang, G., Lv, K., Chen, T., Chen, Z., & Hu, J. (2021). Immobilizing of palladium on melamine functionalized magnetic chitosan beads : A versatile catalyst for p-nitrophenol reduction and Suzuki reaction in aqueous medium. *International Journal of Biological Macromolecules*, *184*, 358–368. https://doi.org/10.1016/j.ijbiomac.2021.06.055

Wu, Y., Wang, D., Zhao, P., Niu, Z., Peng, Q., & Li, Y. (2011). Monodispersed Pd-Ni Nanoparticles: Composition Control Synthesis and Catalytic Properties in the Miyaura - Suzuki Reaction. *Inorganic Chemistry*, *50*, 2046–2048. https://doi.org/10.1021/ic102263b

Xia, J., Fu, Y., He, G., Sun, X., & Wang, X. (2017). Core-shell-like Ni-Pd nanoparticles supported on carbon black as a magnetically separable catalyst for green Suzuki-Miyaura coupling reactions. *Applied Catalysis B: Environmental*, *200*, 39–46. https://doi.org/10.1016/j.apcatb.2016.06.066

Xu, P., Liang, X., Chen, N., Tang, J., Shao, W., Gao, Q., & Teng, Z. (2017). Magnetic separable chitosan microcapsules decorated with silver nanoparticles for catalytic reduction of 4-nitrophenol. *Journal of Colloid And Interface Science*, *507*, 353–359. https://doi.org/10.1016/j.jcis.2017.08.014

Yi, S. S., Lee, D. H., Sin, E., & Lee, Y. S. (2007). Chitosan-supported palladium(0) catalyst for microwave-prompted Suzuki cross-coupling reaction in water. *Tetrahedron Letters*, *48*, 6771–6775. https://doi.org/10.1016/j.tetlet.2007.07.093

Yu, Y., Jung, E., Kim, H. J., Cho, A., Kim, J., Yu, T., & Lee, J. (2020). Protein Particles Decorated with Pd Nanoparticles for the Catalytic Reduction of p - Nitrophenol to p-Aminophenol. *ACS Applied Nano Materials*, *3*(10), 10487–10496. https://doi.org/10.1021/acsanm.0c02406

Zhang, C., Lu, D., Jiang, P., Li, J., & Leng, Y. (2017). Thiol Functionalized Cross-Linked Chitosan Polymer Supporting Palladium for Oxidative Heck Reaction and Reduction of p-Nitrophenol. *Catalysis Letters*, *147*, 2534–2541. https://doi.org/10.1007/s10562-017-2174-6

Zhao, P., Feng, X., Huang, D., Yang, G., & Astruc, D. (2015). Basic concepts and recent advances in nitrophenol reduction by gold- and other transition metal nanoparticles. *Coordination Chemistry Reviews*, *287*, 114–136. https://doi.org/10.1016/j.ccr.2015.01.002

Zinchenko, A., Che, Y., Taniguchi, S., Lopatina, L. I., Sergeyev, V. G., & Murata, S. (2016). Metallization of DNA hydrogel : application of soft matter host for preparation and nesting of catalytic nanoparticles. *Journal of Nanoparticle Research*, *18*(179), 1–9. https://doi.org/10.1007/s11051-016-3480-4